

Imprint effect in PZT thin films at compositions around the morphotropic phase boundary

E. B. Araujo, E. C. Lima, I. K. Bdikin & A. L. Kholkin

To cite this article: E. B. Araujo, E. C. Lima, I. K. Bdikin & A. L. Kholkin (2016) Imprint effect in PZT thin films at compositions around the morphotropic phase boundary, *Ferroelectrics*, 498:1, 18-26, DOI: [10.1080/00150193.2016.1166421](https://doi.org/10.1080/00150193.2016.1166421)

To link to this article: <https://doi.org/10.1080/00150193.2016.1166421>



Published online: 18 May 2016.



Submit your article to this journal [↗](#)



Article views: 159



View Crossmark data [↗](#)



Citing articles: 2 [View citing articles](#) [↗](#)

Imprint effect in PZT thin films at compositions around the morphotropic phase boundary

E. B. Araujo^a, E. C. Lima^b, I. K. Bdikin^c, and A. L. Kholkin^{d,e}

^aFaculdade de Engenharia de Ilha Solteira, UNESP - Univ Estadual Paulista, Departamento de Física e Química, Ilha Solteira, SP, Brazil; ^bUniversidade Federal do Tocantins, Porto Nacional, TO, Brazil; ^cDepartment of Mechanical Engineering & TEMA, University of Aveiro, Aveiro, Portugal; ^dDepartment of Materials and Ceramic Engineering & CICECO, University of Aveiro, Aveiro, Portugal; ^eInstitute of Natural Sciences, Ural Federal University, Russia

ABSTRACT

Piezoresponse force microscopy (PFM) and local piezoresponse hysteresis loops were used to study the imprint effect in $\text{PbZr}_{1-x}\text{Ti}_x\text{O}_3$ thin films at compositions around the morphotropic phase boundary (MPB). Schottky barriers and mechanical coupling between film-substrate were excluded as origin for the imprint in these films. Comparing the composition dependence of the effective d_{33} before poling with some reports in the literature, the existence of point defects such as complex vacancies (V_{Pb} , V_{O} and $V_{\text{Pb}} - V_{\text{O}}$) and Ti^{3+} centers is discussed as probable origin for the imprint effect observed here.

ARTICLE HISTORY

Received 28 June 2015

Accepted 12 November 2015

KEYWORDS

Imprint; PZT; thin films

Introduction

Ferroelectric thin films have been actively studied for the use in nonvolatile ferroelectric random access memories (FeRAM). In the last decades, a crucial issue for the realization of the commercial FeRAMs has been the reliability issue, since degradation effects such as fatigue [1] and imprint [2,3] are responsible for limiting the lifetime and failure of ferroelectric memory devices. The fatigue, the loss of switchable polarization after repeated polarization reversals, is a phenomenon better understood in the literature [4]. On the other hand, the imprint, defined as the tendency of one polarization state to become more stable than the opposite one [5], is a phenomenon more obscure and, for this reason, less understood. In ferroelectric capacitors, the imprint effect is characterized by the asymmetries in the polarization vs. field (P-E) hysteresis loops leading to a failure of stored information [2]. The imprint mechanisms have been often discussed in terms of alignment of defect dipoles and interface screening models for different ferroelectric systems [3,6,7]. Although significant progress has been made in the comprehension of imprint mechanisms in the past, the control of imprint for the purpose of memory applications has motivated recent studies [8,9] maintaining the subject opened for discussions and continuing studies on classical ferroelectrics or new compositions.

CONTACT E. B. Araujo  eudes@dfq.feis.unesp.br

Color versions of one or more of the figures in the article can be found online at www.tandfonline.com/gfer.

© 2016 Taylor & Francis Group, LLC

Among several ferroelectrics, $\text{Pb}(\text{Zr}_{1-x}\text{Ti}_x)\text{O}_3$ (PZT) thin films are still promising candidates for nonvolatile FeRAM and other applications due to their multifunctional properties indispensable for different devices including capacitors [10], piezoelectric transducers [11] and even for THz emission [12]. In the context of imprint effect in ferroelectrics, related phenomenon called self-polarization is often observed in highly textured [13,14] or randomly [15] oriented films. The origin of the self-polarization effect in different ferroelectric systems has been discussed in terms of various mechanisms such as space charge at bottom electrode -film interface [15], asymmetric Schottky barriers, and uncompensated electric field that appear when the bottom and top electrodes are made of different materials [14,16], and mechanical coupling between the film and the substrate [17]. Despite several experiments [18] and proposed theoretical models [19] aimed to explain the mechanisms of the self-polarization effect, its real nature is still an object of intensive discussions.

Recent observation of self-polarization effect in PZT thin films prepared by a polymeric chemical method [20] and the possibility to map the compositional dependence of the imprint effect in these films at compositions around the morphotropic phase boundary (MPB) has motivated the present work. In this study, piezoresponse force microscopy (PFM) measurements and local piezoresponse hysteresis loops have been used to study the compositional dependence of the imprint effect in PZT thin films.

Experimental

Using a polymeric resin prepared by a chemical method based on the Pechini method, $\text{PbZr}_{1-x}\text{Ti}_x\text{O}_3$ (PZT) thin films at the compositions $x = 0.46, 0.47, 0.48, 0.49$ and 0.50 were deposited by spin coating on $\text{Pt}(111)/\text{Ti}/\text{SiO}_2/\text{Si}$ substrates. To compensate the loss of lead during the film crystallization and to stabilize the growth of the perovskite phase, each nominal composition was prepared with 10 mol% of lead in excess. Details about the polymeric resin preparation are described elsewhere [21]. To remove organics, each as-deposited film was pyrolyzed at 300°C for 30 min and then crystallized at 700°C for 1 h. All final films were ~ 710 nm in thickness, being homogeneous and crack-free.

Modified commercial atomic force microscopes (AFM) (Multimode, Nanoscope III, Bruker and Ntegra Aura, NT-MDT) were used to obtain the PFM data of the studied films. Nitrogen doped Si tips were used with a spring constant 42 N/m to avoid possible electrostatic effects.

Results and discussion

Local piezoresponse hysteresis is indeed useful to map the polarization asymmetry within the individual grain and it is sensitive only to the top surface due to the localized nature of applied electric field by the PFM tip. Figure 1(a) shows the local piezoresponse hysteresis loops (averaged at several locations) of PZT films of different compositions. Analogously to P-E hysteresis loops, we plot in Figure 1(b) the differences $\Delta d_{33} = d_{33}^+ - d_{33}^-$ and $\Delta V_c = V_c^+ - V_c^-$ as a function of the composition to reveal the asymmetries on the local hysteresis. In this Figure, the asymmetry of the coercive voltage is almost zero for all compositions ($\Delta V_c \cong 0$), while Δd_{33} exhibits a positive maximum ($\Delta d_{33} > 0$) for $x = 0.48$ and a negative value ($\Delta d_{33} < 0$) for $x = 0.50$ and 0.46 . Again, a strong shift of the effective d_{33} loops is apparently observed for compositions $x = 0.48$ and 0.50 , also reflecting the presence

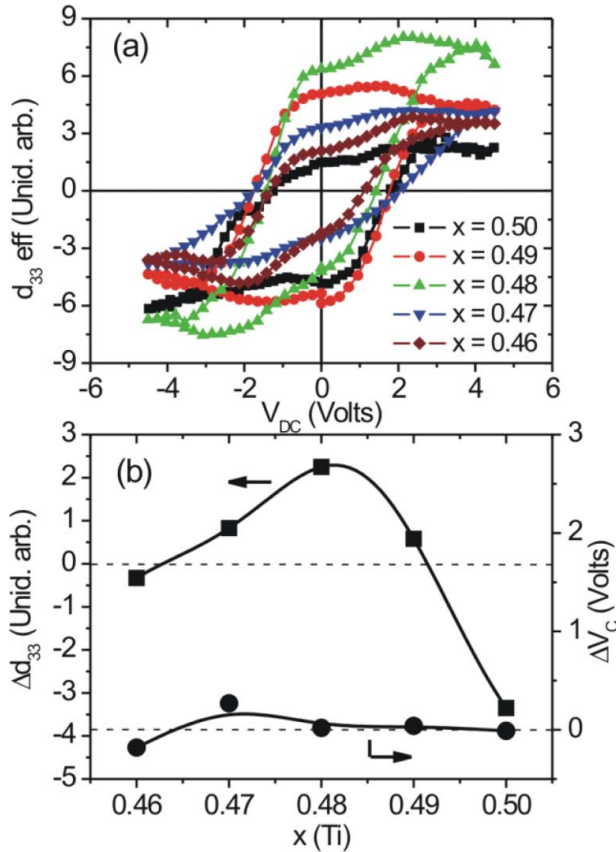


Figure 1. (a) Local piezoresponse hysteresis loops and (b) behavior of the vertical ($\Delta d_{33} = d_{33}^+ - d_{33}^-$) and horizontal ($\Delta V_c = V_c^+ - V_c^-$) shifts of the loops as a function of PZT composition. Lines are drawn as a guide to the eye.

of self-polarization effect at the nanoscale. However, the trend in the compositional behavior of coercive voltages is completely different. It can be related to the fact that the coercive voltage in the PFM experiment is not a real one and is related to equal contributions from the nascent domain and the rest of the film²² and thus several contributions can affect this behavior. In addition, it is related only to the surface layer, whereas macroscopic effect is a result of the bulk contribution. Apparently, the compositional dependence of Δd_{33} is very close to polarization. It means that relaxation of piezoelectric coefficient in quasistatic d_{33} measurements is very close to dynamic relaxation in P-E curves and no polarization offset due to frozen domains is present.

Figure 2(a) shows the topography images of PZT films of different compositions. The morphology of the studied films is very similar for all compositional range. This result suggests that surface morphology of the studied PZT films is not affected by the Ti concentration in the studied range. The RMS roughness parameter, defined as the standard deviation of the surface height within a given area, has been used to describe the surface morphology of AFM height images. The average RMS roughness of the films shows essentially the same value around 31 nm, while the average grain size of these was around 77 nm. Figure 2(b) shows the piezoresponse images of the films with different compositions. In all images, a

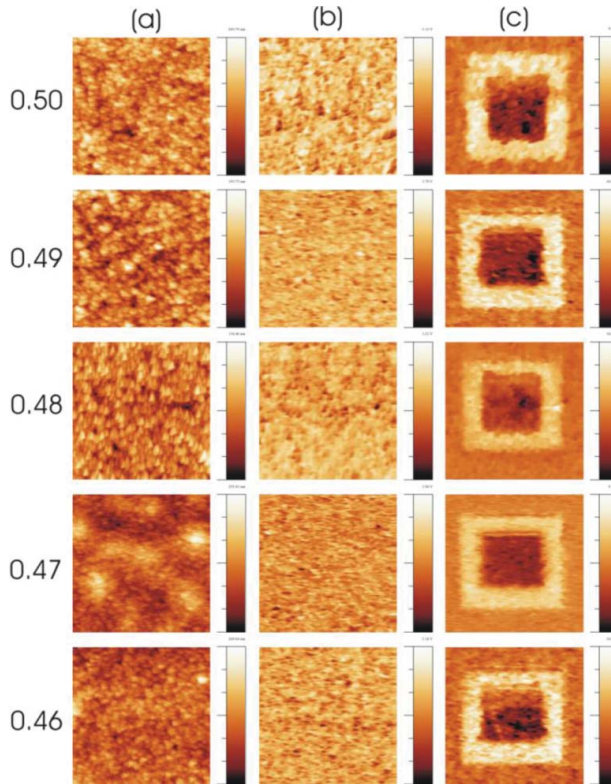


Figure 2. (a) Topography, (b) piezoresponse of upoled and (c) of poled $\text{Pb}(\text{Zr}_{1-x}\text{Ti}_x)\text{O}_3$ thin films of the compositions $x = 0.46, 0.47, 0.48, 0.49$ and 0.50 . Scale of all images is $10 \times 10 \mu\text{m}^2$.

predominance of the dark contrast (negative d_{33}) over bright contrast was revealed, indicating that “negative” domains (polarization head directed toward the bulk of the film) are predominant over “positive” domains. **Figure 2(c)** summarizes the out-of-plane images of the same PZT films after poling by the PFM tip. They reflect two antiparallel polar states in the ferroelectric films, which were induced by the application of a dc voltage of $+30 \text{ V}$ in the white area and -30 V in the dark area and subsequent imaging.

Figure 3(a) shows the histograms of the local piezoresponse of PZT films of different compositions. The distributions curves in this Figure were calculated based on piezoresponse images of unpoled and poled films shown in **Figure 2(b)** and **2(c)**, respectively. In **Figure 3 (a)**, the single peak (closed squares) refers to the local piezoresponse before poling, while two peaks after poling (open squares) are associated with reoriented polar states and their positions can be roughly considered as average values of the intrinsic piezoresponse inside poled region. The shift to the negative values observed for the single d_{33} peak before poling in **Figure 3(a)** confirms once again the existence of a self-polarization effect at the nanoscale. It should be noted that the distribution of piezoelectric coefficient could be affected by electrostatic response described by following equation [23]:

$$A_{\omega_1} \cos \Phi_{\omega_1} = d_{33}^{\text{eff}} V_{ac} + \frac{\partial C}{\partial z} (V_{dc} - V_s) V_{ac}$$

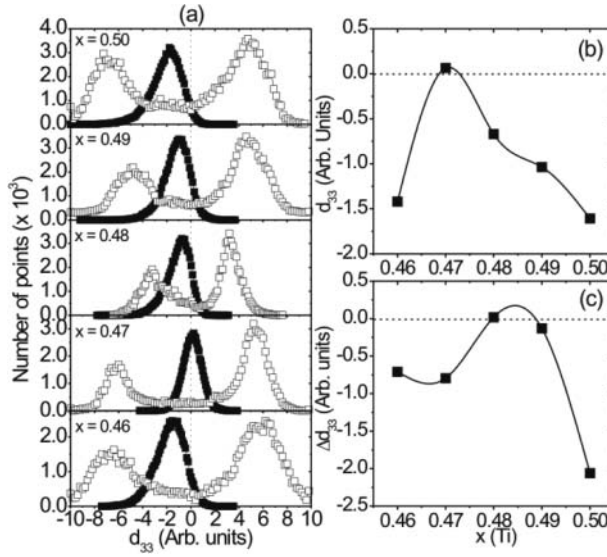


Figure 3. (a) Distribution of the local piezoresponse before poling (black curves) and after poling (white curves) for different compositions of PZT films with 710 nm in thickness. (b) Compositional dependence of the effective d_{33} before poling. (c) Compositional dependence of $\Delta d_{33} = d_{33}^+ - d_{33}^-$ after poling. Lines are drawn as a guide to the eye.

where $A_{\omega 1}$ is the amplitude of acquired response, $\Phi_{\omega 1}$ is the phase, V_{ac} is the applied ac voltage, d_{33}^{eff} is the effective piezoelectric coefficient, C is the capacitance of the system PFM tip-sample-bottom-electrode, V_{dc} is the applied bias, and V_s is the contact potential difference between the tip and ferroelectric surface. The first term in this equation is the true piezoelectric contribution whereas the second term is the capacitive part of the cantilever. Even if V_{dc} is zero, the second term is always present as an offset that can vary with the composition of the films.

Based on the Figure 3(a), we plot the compositional dependences of the effective d_{33} before poling and difference $\Delta d_{33} = d_{33}^+ - d_{33}^-$ between d_{33} peaks after poling in Figures 3(b) and 3(c), respectively. The d_{33} shift from zero before poling indicates again the existence of an internal bias field in the films while the difference Δd_{33} reflect the asymmetry of the effective d_{33} peaks around zero between the two polar states after poling. The d_{33} shift observed for negative values in Figure 3(b) confirms the imprint effect at PZT films with different compositions, and this effect tend to disappear for $x = 0.47$ where $d_{33} \approx 0$. On the other hand, Figure 3(c) clearly indicates $\Delta d_{33} \approx 0$ at compositions $x = 0.48$ and 0.49 , leading to almost symmetrical d_{33} peaks for these compositions.

The imprint effect in ferroelectric films has been a subject of numerous studies in the literature and is explained considering different models [6,24]. As a direct manifestation of the imprint behavior in highly oriented ferroelectric thin films, self-polarization effect has been explained either in terms of Schottky barrier at the bottom interface [14,15] or due to a mechanical coupling between the ferroelectric film and substrate [17]. Asymmetric Schottky barriers appear when the bottom and top electrodes are made of different materials [16], while mechanical coupling is associated with the presence of a compressive/tensile stress or different thermal expansion coefficients between the film and the substrate. Recent studies on the thickness dependence of imprint in PZT films prepared by the same method used in

the present work definitively excluded Schottky barriers and mechanical coupling near the film-substrate interface as mechanisms responsible for the self-polarization in these films [25]. This information is an important starting point to understand the compositional dependence of the imprint-related parameters studied in the present work.

Excluding trapped charges near the bottom ferroelectric-electrode interface as the dominant mechanism responsible by the imprint effect in our films, it is now opportune to discuss the results in view of the proposed models in the literature. The photo [7] and thermally [3] induced voltage/polarization shifts in ferroelectric capacitors or bulk ceramics have been interpreted in terms of defect dipole and bulk screening models [6,24]. The defect dipole model assumes that controlling the oxygen pressure on the sample during the crystallization/sintering or introducing donor/acceptor impurities in the sample, new species such as oxygen vacancies ($V_{\text{O}}^{\cdot\cdot}$) and cation vacancies ($V_{\text{A}}^{\cdot\cdot}$) are generated in the perovskite ABO_3 structure [6]. The addition of donor dopants to this structure (e.g. Nb) leads to substitution at B sites and significant reduction of the thermally induced voltage shifts in PZT films. In such cases, the addition of donor dopants reduces the concentration of oxygen vacancies, thereby reducing the voltage shifts in P-E hysteresis loops. In addition, it is assumed that the complexes defect-dipole such as lead vacancy-oxygen vacancy ($V_{\text{Pb}}^{\cdot\cdot} - V_{\text{O}}^{\cdot\cdot}$) in PZT films are present due to PbO loss during synthesis by using chemical methods like sol-gel. Then, it is expected that these defects also contribute to the thermally induced voltage shifts observed in PZT films.

The screening model also explains imprint in ferroelectric films in terms of electric charges in a thin surface layer [24]. Different mechanisms have been proposed in the literature to explain the existence of a surface layer in ferroelectric materials, which is responsible for the imprint effect. In a comprehensive review, Grossmann *et al.* [6] showed that no spontaneous polarization is present in the surface layer and, based on the model proposed by Dimos *et al.* [24], the residual depolarizing field causes a charge separation in the surface layer. Using PFM technique to explore the photoinduced changes in individual grains of PbTiO_3 films, Gruverman *et al.* [7] suggested that an electric field in a thin layer at the film surface is responsible for the voltage shifts in hysteresis loops and electronic carriers trapped in the bulk of the film do not contribute to the voltage shift. In addition, recent modifications of the boundary conditions in the Landau-type approach demonstrated that the surface of ferroelectric thin films is itself a defect leading to an electric field that smear out the ferroelectric phase transition [26]. Despite the different origins for this electric field, it is a consensus that high defect density in the top surface plays a significant role in domain pinning [7], imprint effect [6] and phase transition smearing [26] in ferroelectric films.

Considering the scenario described in above paragraphs, the imprint behavior in our PZT films is qualitatively understood. Assuming the existence of a surface layer in these PZT films, the equivalent capacitance (C_{eq}) can be represented by a ferroelectric capacitor (C_f) in series with a surface capacitor (C_s) such as $C_{eq} = C_f C_s / (C_s + C_f)$, where C_f depends on the film thickness d such as $C_f \propto (d - \delta)^{-1}$ while $C_s \propto \delta^{-1}$. Considering that the thickness δ of the surface layer is independent and much smaller than the film thickness d ($\delta \ll d$), a smaller dielectric permittivity is expected for this film if compared to bulk ceramics or films with the surface layer effect minimized. In fact, the dielectric permittivity ($\epsilon \sim 460$) of the PZT films [25] in this work is smaller than observed for other PZT films in the literature ($\epsilon \sim 1310$) prepared by sol-gel at compositions near MPB [27].

Then, the lower dielectric permittivity in the studied PZT films suggests an existence of a surface layer in our films.

The compositional dependence of the effective d_{33} shift shown in Figure 3(b) can be now discussed in terms of a compositional dependence of bulk Ti^{3+} centers, and defects associated with oxygen vacancies, lead vacancies and complexes lead vacancy-oxygen vacancy [3]. Due to lead excess introduced during the synthesis, the oxygen vacancies in PZT thin films appear during the annealing in high-temperature for the perovskite phase formation. In this case, it is expected that oxygen vacancy ($V_{\text{O}}^{\cdot\cdot}$) density increase for Ti-rich compositions, leading to a lower thermally induced voltage shift for Zr-rich compositions. This is not the case observed in Figure 3(b). On the other hand, theoretical and electron paramagnetic resonance measurements [28] in PZT powders demonstrated that activated Pb^{3+} centers are relatively independent of Zr content in PZT, but activated Ti^{3+} centers, due to electron trapped such as $\text{Ti}^{4+} + e^- \rightarrow \text{Ti}^{3+}$, exhibit a pronounced maximum density at around the composition $x = 0.47$ with Ti^{3+} densities decreasing to Zr-rich and Ti-rich compositions. As shown in Figure 3(b), we observed a minimum d_{33} shift at around the PZT composition $x = 0.47$ while d_{33} shifts increases for negative values for both Zr-rich and Ti-rich compositions. Then, this result suggests a strong relationship between d_{33} shift observed for different compositions and Ti^{3+} centers in the studied films. Considering higher mobility of Pb^{2+} ions relative to O^{2-} ions during the film processing, such as suggested by Watts *et al.* [29], it is reasonable assume that defects such as oxygen vacancies $V_{\text{O}}^{\cdot\cdot}$, lead vacancies $V_{\text{Pb}}^{\cdot\cdot}$ and probably complex dipoles $V_{\text{Pb}}^{\cdot\cdot}-V_{\text{O}}^{\cdot\cdot}$ are introduced at the film surface during the synthesis, *independently* of the composition. Assuming the existence of these complex defects, we can explain the imprint effect observed in our films. However, probably the origin of the imprint effect is not only due to these defects. The compositional dependence of the imprint shown in Figure 3(b), with no perceptible d_{33} shift at $x = 0.47$, suggests that a combined effect due to the complex vacancies and Ti^{3+} centers decreases the effective charge at the film surface at around the MPB region, where the Ti^{3+} density increases. Consequently, the effective electric field due to the complex vacancies ($V_{\text{Pb}}^{\cdot\cdot}$, $V_{\text{O}}^{\cdot\cdot}$ and $V_{\text{Pb}}^{\cdot\cdot}-V_{\text{O}}^{\cdot\cdot}$) and Ti^{3+} centers is minimized at around the composition $x = 0.47$ leading to a pronounced reduction in the d_{33} shift, as observed in Figure 3(b). Complex interplay of the surface defects, band bending at the surface, and tip-induced electrostatic effects is probably responsible for the non-monotonous variation of the histogram parameters presented in Figure 3. Further experiments (e.g. Kelvin Probe Force Microscopy, KPFM) are needed to uncover the origin of this behavior.

Conclusions

In summary, we studied the imprint behavior in PZT thin films prepared by chemical method at compositions around MPB. Asymmetries on the local piezoresponse hysteresis loops and piezoresponse distribution confirm the imprint effect in the studied films. Excluding Schottky barriers and mechanical coupling between film-substrate, and comparing the maximum observed for effective d_{33} before poling at the composition $x = 0.47$ with reports in the literature, the existence of point defects such as complex vacancies ($V_{\text{Pb}}^{\cdot\cdot}$, $V_{\text{O}}^{\cdot\cdot}$ and $V_{\text{Pb}}^{\cdot\cdot}-V_{\text{O}}^{\cdot\cdot}$) and Ti^{3+} centers has been discussed as probable origin for the imprint effect observed here.

Funding

We would like to express our gratitude to the Brazilian agencies FAPESP (Projects N° 2010/16504-0 and 2007/08534-3) and CNPq (Research grant 305973/2012-6 and Project N° 400677/2014-8) for their financial support. Center for Research on Ceramic and Composite materials (CICECO) of the University of Aveiro (PEst-C/CTM/LA0011/2013) is also acknowledged for the support.

References

1. J. F. Scott, and C. A. P. Araujo, Ferroelectric memories. *Science* **246**, 1400–1405 (1989).
2. W. L. Warren, D. Dimos, G. E. Pike, B. A. Tuttle, M. V. Raymond, R. Ramesh, and J. T. Evans, Voltage shifts and imprint in ferroelectric capacitors. *Appl. Phys. Lett.* **67**, 866–868 (1995).
3. W. L. Warren, B. A. Tuttle, D. Dimos, G. E. Pike, H. S. Al-Shareef, R. Ramesh, and J. T. Evans Jr, Imprint in ferroelectric capacitors. *Jpn. J. Appl. Phys.* **35**, 1521–1524 (1996).
4. A. K. Tagantsev, I. Stolichnov, E. L. Colla, and N. Setter, Polarization fatigue in ferroelectric films: Basic experimental findings, phenomenological scenarios, and microscopic features. *J. Appl. Phys.* **90**, 1387–1402 (2001).
5. H. N. Al-Shareef, D. Dimos, W. L. Warren, and B. A. Tuttle, Voltage offsets and imprint mechanism in SrBi₂Ta₂O₉ thin films. *J. Appl. Phys.* **80**, 4573–4577 (1996).
6. M. Grossmann, O. Lohse, D. Bolten, U. Boettger, T. Schneller, and R. Waser, The interface screening model as origin of imprint in PbZr_xTi_{1-x}O₃ thin films. I. Dopant, illumination, and bias dependence. *J. Appl. Phys.* **92**, 2680–2687 (2002).
7. A. Gruverman, B. J. Rodriguez, R. J. Nemanich, and A. I. Kingon, Nanoscale observation of photoinduced domain pinning and investigation of imprint behavior in ferroelectric thin films. *J. Appl. Phys.* **92**, 2734–2739 (2002).
8. T. Morita, Y. Kadota, and H. Hosaka, Shape memory piezoelectric actuator. *Appl. Phys. Lett.* **90**, 082909 (2007).
9. W. H. Kim, J. Y. Son, Y. H. Shin, and H. M. Jang, Imprint control of nonvolatile shape memory with asymmetric ferroelectric multilayers. *Chem. Mater.* **26**, 6911–6914 (2014).
10. M. Miyake, J. F. Scott, X. J. Lou, F. D. Morrison, T. Nonaka, S. Motoyama, T. Tatsuta, and O. Tsuji, Submicron three-dimensional trenched electrodes and capacitors for DRAMs and FRAMs: Fabrication and electrical testing. *J. Appl. Phys.* **104**, 064112 (2008).
11. T. Maeder, P. Murali, L. Sagalowicz, I. Reaney, M. Kohli, A. Kholkin, and N. Setter, Pb(Zr,Ti)O₃ thin films on zirconium membranes for micromechanical applications. *Appl. Phys. Lett.* **68**, 776–778 (1996).
12. J. F. Scott, H. J. Fan, S. Kawasaki, J. Banys, M. Ivanov, A. Krotkus, J. Macutkevicius, R. Blinc, V. V. Laguta, P. Cevc, J. S. Liu and A. L. Kholkin, Terahertz Emission from Tubular Pb(Zr,Ti)O₃ Nanostructures. *Nano Lett.* **8**, 4404–4409 (2008).
13. I. Kanno, S. Fujii, T. Kamada, and R. Takayama, Piezoelectric properties of c-axis oriented Pb(Zr, Ti)O₃ thin films. *Appl. Phys. Lett.* **70**, 1378 (1997).
14. A. L. Kholkin, K. G. Brooks, D. V. Taylor, S. Hiboux, and N. Setter, Self-polarization effect in Pb(Zr,Ti)O₃ thin films. *Integr. Ferroelectr.* **22**, 525–533 (1998).
15. V. P. Afanasjev, A. A. Petrov, I. P. Pronin, E. A. Tarakanov, E. J. Kaptelov, and J. Graul, Polarization and self-polarization in thin PbZr_{1-x}Ti_xO₃ (PZT) films. *J. Phys-Condens. Mat.* **13**, 8755–8763 (2001).
16. D. Dawber, K. M. Rabe, and J. F. Scott, Physics of thin-film ferroelectric oxides. *Rev. Mod. Phys.* **77**, 1083–1130 (2005).
17. A. Gruverman, B. J. Rodriguez, A. I. Kingon, R. J. Nemanich, A. K. Tagantsev, J. S. Cross, and M. Tsukada, Mechanical stress effect on imprint behavior of integrated ferroelectric capacitors. *Appl. Phys. Lett.* **83**, 728–730 (2003).
18. V. P. Afanasjev, I. P. Pronin, and A. L. Kholkin, Formation and relaxation mechanisms of the self-polarization in thin ferroelectric films. *Phys. Solid State* **48**, 1214–1218 (2006).
19. A. K. Tagantsev, and G. Gerra, Interface-induced phenomena in polarization response of ferroelectric thin films. *J. Appl. Phys.* **100**, 051607 (2006).

20. E. C. Lima, E. B. Araujo, A. G. Souza Filho, A. R. Paschoal, I. K. Bdikin, and A. L. Kholkin, Structural depth profile and nanoscale piezoelectric properties of randomly oriented $\text{Pb}(\text{Zr}_{0.50}\text{Ti}_{0.50})\text{O}_3$ thin films. *J. Phys. D: Appl. Phys.* **45**, 215304 (2012).
21. E. C. Lima, and E. B. Araujo, *Adv. Mater. Phys. Chem.* **2**, 178 (2012).
22. A. Wu, P. M. Vilarinho, V. V. Shvartsman, G. Suchanek, and A. L. Kholkin, Domain populations in lead zirconate titanate thin films of different compositions via piezoresponse force microscopy. *Nanotechnology* **16**, 2587–2595 (2005).
23. S. Hong, J. Woo, H. Shin, J. U. Jeon, Y. E. Pak, E. L. Colla, N. Setter, E. Kim, and K. No, Principle of ferroelectric domain imaging using atomic force microscope. *J. Appl. Phys.* **89**, 1377–1386 (2001).
24. D. Dimos, W. L. Warren, M. B. Sinclair, B. A. Tuttle, and R. W. Schwartz, Photoinduced hysteresis changes and optical storage in $(\text{Pb},\text{La})(\text{Zr},\text{Ti})\text{O}_3$ thin-films and ceramics. *J. Appl. Phys.* **76**, 4305–4315 (1994).
25. E. B. Araujo, E. C. Lima, I. K. Bdikin, and A. L. Kholkin, Thickness dependence of structure and piezoelectric properties at nanoscale of polycrystalline lead zirconate titanate thin films. *J. Appl. Phys.* **113**, 187206 (2013).
26. A. M. Bratkovsky, and A. P. Levanyuk, Smearing of phase transition due to a surface effect or a bulk inhomogeneity in ferroelectric nanostructures. *Phys. Rev. Lett.* **94**, 107601 (2005).
27. H. D. Chen, K. R. Udayakumar, C. J. Gaskey, and L. E. Cross, Electrical-properties maxima in thin-films of the lead zirconate lead titanate solid-solution system. *Appl. Phys. Lett.* **67**, 3411–3413 (1995).
28. J. Robertson, W. L. Warren, and B. A Tuttle, Band states and shallow hole traps in $\text{Pb}(\text{Zr},\text{Ti})\text{O}_3$ ferroelectrics. *J. Appl. Phys.* **77**, 3975–3980 (1995).
29. B. E. Watts, F. Leccabue, G. Tallarida, S. Ferrari, M. Fanciulli, and G. Padeletti, Surface segregation mechanisms in dielectric thin films. *Integr. Ferroelectr.* **62**, 3–11 (2004).